Size and concentration effects of gold nanoparticles on the plasmonic sensing of Cr(VI)

Kirana Yuniati Putri[1], *Lindu Dwi* Kinanti[2], *Nurfina* Yudasari[1], *Yuliati* Herbani[1], and *Dede* Djuhana[3, *]

[1]Research Center for Photonics, National Research and Innovation Agency (BRIN), KST BJ Habibie, South Tangerang, Banten 15314, Indonesia
[2]Department of Physics, Faculty of Mathematics and Natural Sciences (FMIPA), Universitas Andalas, Padang, West Sumatera 25163, Indonesia
[3]Department of Physics, Faculty of Mathematics and Natural Sciences (FMIPA), Universitas Indonesia, Depok 16424, Indonesia

Abstract. It is very important to determine the presence of toxic Cr(VI) in aqueous environment. Detection of Cr(VI) using AuNPs has been carried out based on the oxidation or etching principle, which results in the change of localized surface plasmon resonance. In this work, the effects of size and concentration of colloidal AuNPs on the Cr(VI) sensing characteristics were studied by both simulation and experiment. In the simulation study using MNPBEM toolbox, the etching process was described as shrinking of AuNPs with total volume loss reflecting the concentration of Cr(VI) as oxidizing ions. The experiment was carried out by exposing colloidal AuNPs with different size and concentration to Cr(VI). The AuNPs were obtained from laser-induced photochemical process, in which aqueous solution of Au ions were subjected to femtosecond laser irradiation. The simulation results showed wider blue-shift of λ_{LSPR} per total volume loss when larger AuNPs were employed and higher intercept value of extinction decrease per total volume loss when more AuNPs were present in the system. Correspondingly, the experiment demonstrated more distinct color change and wider λ_{LSPR} per Cr(VI) concentration when larger AuNPs were used. More concentrated colloid showed still-red color after Cr(VI) etching, representing higher intercept value of extinction decrease per Cr(VI). Both simulation and experiment results show that, in etching-based Cr(VI) sensing, large AuNPs displayed wider LSPR wavelength shift compared to the small nanoparticles. On the other hand, concentration of AuNPs contributes to the intensity change and higher concentration of AuNPs offers higher Cr(VI) sensing range. This result provided an insight on how colorimetric sensor performance might be affected by the choice of nanoparticle size and concentration used in the system.

Keywords. Gold nanoparticles, plasmonic sensor, chromium

*Corresponding author: dede.djuhana@sci.ui.ac.id

1 Introduction

Chromium is a transitional metal known for existing with several oxidation states in water. The most stable states are trivalent chromium (Cr(III)) and hexavalent chromium (Cr(VI)). Cr(VI) is extremely toxic and has been associated with various health problems, which depend on dose, exposure level, and duration [1]. Prolonged exposure of Cr(VI) can lead to serious health problems such as skin irritation, hemolysis, liver failure, kidney damage, and various types of cancer. Global concerns related to the environmental contamination of Cr(VI) are increasing and limitation of how much Cr(VI) is allowed in drinking water has been made. To ensure compliance with the safety threshold, it is essential to identify the presence of Cr(VI).

Detection of Cr(VI) has been performed by various conventional techniques, such as inductively coupled plasma mass spectrometry (ICP-MS) [2], atomic absorption spectroscopy (AAS) [3], X-ray fluorescence (XRF) [4], which are often costly, complicated, and impossible to be performed in-situ. Recently, there is growing interest in the use of gold nanoparticles (AuNPs) for the colorimetric detection of Cr(VI) owing to the simple procedure and easier observation [5, 6]. They possess a unique property namely localized surface plasmon resonance (LSPR), which corresponds to the color of the colloidal solution [7]. LSPR involves the collective oscillation of free electrons in metallic nanoparticles when they are exposed to electromagnetic radiation. LSPR is highly sensitive to the change in the environment surrounding nanoparticles and can be tuned by modifying the size, shape, or composition of the nanoparticles.

Colorimetric sensing of Cr(VI) using AuNPs often employs analyte-induced aggregation mechanism, which involves the reduction of Cr(VI) to Cr(III) in the process [5, 6]. An alternative direct detection of Cr(VI) has been made possible by the fact that Cr(VI) is able to oxidize AuNPs in the presence or bromide ions [8, 9]. The leaching process causes the AuNPs to change shape and/or size, leading to the LSPR shift. The detection mechanism of such sensors has been studied extensively, including the prospect of using different shape of AuNPs. However, there is not much information on how the size and concentration of AuNPs may affect the detection performance. The geometrical parameters allow maximizing of color difference upon nanoparticle aggregation [10]. AuNP size also played an important role in the colorimetric detection of nickel ions (Ni(II)) [11]. In this work, we studied the characteristic of leaching-based Cr(VI) sensing using AuNPs with different size and concentration. We made our approach through simulation study and experiment. Both the simulation and experiment result demonstrated the different trends of LSPR change in relation with the size and concentration of colloidal AuNPs.

2 Methods

2.1 Simulation study

MNPBEM toolbox was used to simulate the size and concentration effect of AuNPs to the Cr(VI) sensing characteristics. MNPBEM is a Matlab toolbox specifically designed for modelling the electromagnetic properties of metallic nanoparticles (MNP) using a boundary element method (BEM). Details regarding the toolbox has been described elsewhere [12, 13]. In brief, MNPBEM solves Maxwell's equations for dielectric environment consisting of dielectric bodies with homogenous dielectric properties separated by immediate boundaries, which represents the nanoparticles suspended in medium (Fig. 1a). In our investigation, the nanoparticle was defined as spherical AuNPs in water medium (refractive index nm = 1.33). The dielectric constant of Au was taken from Johnson and Christy [14]. To illustrate the

etching-based sensing of Cr(VI), a series of MNPBEM simulation was performed on the AuNPs with decreasing size (Fig. 1b). The increasing total volume loss in every decrement step corelated to the increasing total oxidized volume of AuNPs and further corresponded to the increasing concentration of Cr(VI) in the system. After assigning the 'comparticle' object and excitation conditions, BEM solver was called to compute the surface charge as well as calculated the extinction cross section for a given excitation. 'Comparticle' objects defined the positions of particles in the medium.

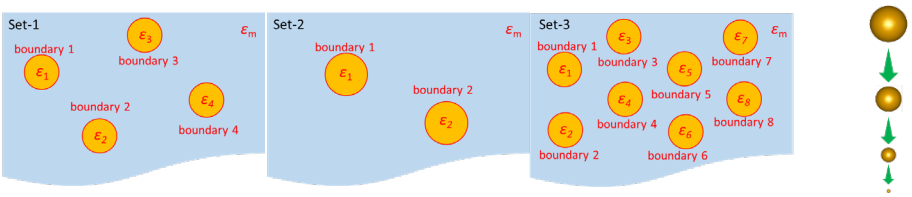

Fig. 1. (a) The representative models of AuNPs in a water medium. (b) Decreasing size of AuNPs represented the etching-based Cr(VI) sensing.

To simulate the size effect, two sets of objects were modeled. One set was composed of 28.8 nm particles (Set-1), while the other consisted of larger particles with sizes of 36.3 nm (Set-2). The particle sizes were set to be sufficiently large for multi-step etching yet still close to the commonly used size [5]. The number of particles in each model was adjusted so that their total particle volumes (V_T) were equal, representing the same Au concentration in both systems. Next, to explore the effect of Au concentration, an additional set of objects (Set-3) was prepared, containing 28.8 nm particles whose total volume was twice as much as Set-1. Three size-decreasing steps, with same total volume loss (V_L) of 10,000 nm^3 for each model, were set to mimic the use of three different concentration of etching-inducing analyte. The optical responses for all three models were then compared.

2.2 Experimental

Spherical AuNPs were prepared according to the femtosecond laser-induced photochemical reduction method, which has been described elsewhere [15, 16]. Figure 2 illustrates the experimental setup, which consists of femtosecond laser, focusing system, and UV-visible absorption monitoring system. To produce AuNPs, 3 mL precursor solution containing Au(III) ions was subjected to femtosecond laser beam (800 nm, 100 fs, 1 kHz, 1.8 mJ) delivered by a Ti:saphhire-based amplifier (Spitfire Ace, Spectra Physics). The Au solution were prepared at 0.125 mM and 0.25 mM by proper dissolution of potassium tetrachloroaurate(III) (KAuCl4, 99.99 %, Sigma-Aldrich) with aquabidest. Interaction between laser and water generates various reactive species capable of reducing Au(III) ions. The laser irradiation time was adjusted to 15 and 5 minutes for the 0.125 mM Au^{3+} solution (Exp-1 and Exp-2), while the 0.25 mM Au^{3+} solution was irradiated for 15 minutes (Exp-3). Before and after irradiation, the UV-visible extinction spectrum of each sample was recorded by the self-built UV-visible absorption measurement system. The system consisted of a deuterium-halogen light source (Ocean Optics, DH-mini), fiber optics, collimators, and a portable spectrophotometer (Ocean Optics, Maya2000Pro) connected to a processing unit.

The obtained AuNPs from the laser-induced photochemical process were then stabilized using bovine serum albumin (BSA, Sigma-Aldrich). An aliquot of BSA solution (50 µM, 50 µL) was added to the colloidal AuNPs and equilibrated for 30 minutes

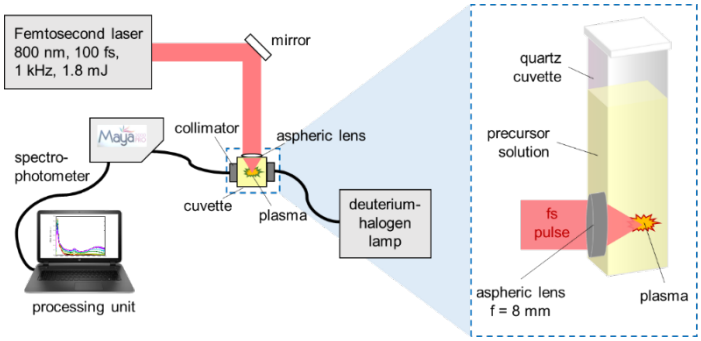

Fig. 2. Experimental setup.

in room temperature. The Cr(VI) sensing procedure started with adding 20 µL of 8.0 hydrobromic acid (HBr, Merck) into BSA-AuNPs solution. Various volumes of 1 mM Cr(VI) were then added, resulting in final Cr(VI) concentration of 28.57 µM, 57.14 µM, 85.71 µM, and 114.28 µM. The final volume of each test solution was fixed at 3.5 mL by adding a proper volume of aquabidest. After equilibrated for 5 minutes, the UV-Vis extinction spectrum of each sample was recorded.

3 Results and discussion

The results of simulation study for colloidal AuNPs with various size and concentration are shown in Fig. 3. At the same V_T of 50,100 nm, the extinction cross sections of initial AuNPs in Set-1 and Set-2 were nearly equivalent. However, the LSPR peak wavelengths (λ_{LSPR}) were slightly shifted, from 524 nm for Set-1 to 526 nm for Set-2. The size-affected LSPR shift trend is well known [7]. Larger AuNPs have a greater volume and a larger number of conduction electrons, thus decreasing the electron oscillation frequency (resonance frequency). On the other hand, the initial extinction cross section exhibits by Set-3 was almost twice higher than the others. Yet, the λ_{LSPR} was similar to Set-1 (524 nm). This phenomenon represents the higher likelihood of light-matter interaction with increasing number of particles [7]. When etching steps were applied, these extinction spectra changed.

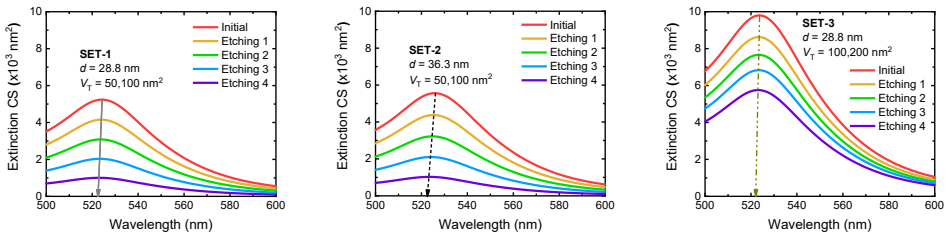

Fig. 3. Extinction spectra from etching simulation using different sets of AuNPs: (a) small size and low concentration, (b) big size and low concentration, (c) small size and high concentration.

Figure 4a and 4b shows the λ_{LSPR} and extinction cross section as functions of V_L. The λ_{LSPR} shift per volume loss ($\Delta\lambda_{LSPR}$ /V_L) was determined to be 3.5 × 10^{-5} nm^{-2}, 6.0 × 10^{-5} nm^{-2}, and 1.0 × 10^{-5} nm^{-2} for Set-1, Set-2, and Set-3 respectively. Higher $\Delta\lambda_{LSPR}$ /V_L shown by Set-2 suggested better resolution, so more color change might be observed during etching-based detection of Cr(VI) using large AuNPs. Meanwhile,

the extinction cross section decreases per volume loss ($\Delta ECS/V_L$) were calculated to be 0.106/nm^3, 0.113/nm^3, and 0.098/nm^3 for Set-1, Set-2, and Set-3, respectively. Their respective intercept values were 5.2 × 10^3, 5.5 × 10^3, and 9.7 × 10^3. The $\Delta ECS/V_L$ values were similar, which attributed to the similar total volume loss in every etching step for each model. This result indicated that AuNP concentration does not significantly affect the color intensity change. However, the higher intercept value exhibited by Set-3 might allow higher number of etchings performed, i.e. lower detection limit.

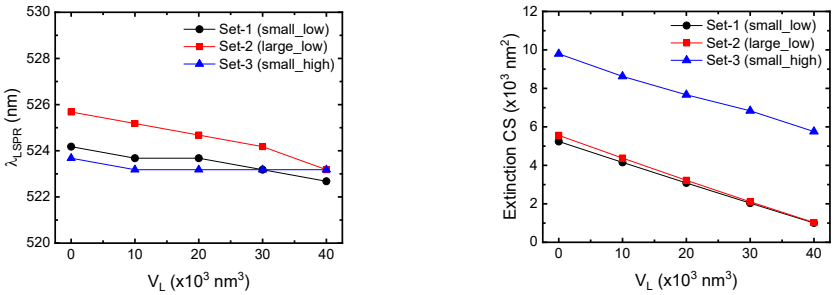

Fig. 4. (a) LSPR wavelength and (b) extinction cross section as a function of total volume loss.

Five and fifteen minutes of femtosecond laser irradiation were sufficient to fully reduce 0.125 mM and 0.25 mM Au(III) ions in water. The recorded extinction spectra for the three samples (Exp-1, Exp-2, and Exp-3) are shown in Fig. 5a. Single LSPR peak suggesting the existence of spherical AuNPs. The λ_{LSPR} values were 512 nm, 521 nm, and 515 nm for Exp-1, Exp-2, and Exp-3, respectively. Their respective measured extinctions were 0.365, 0.433, and 0.843. This result supported the abovementioned simulation results. At the same Au concentration, larger particles showed redshifted λ_{LSPR} and slightly increasing extinction. On the other hand, more concentrated particles showed much higher extinction but without significant λ_{LSPR} shift. The high extinction peak showed by Exp-3 sample contributed to its intense red color. According to Khlebtsov [17], the AuNP size can be estimated from its λ_{LSPR} using following equation.

$$d = \begin{cases} 3 + 7.5 \times 10^{-5} X^4, & X < 23 \\ (\sqrt{X - 17} - 1)/0.06, & X \geq 23 \end{cases} \qquad X = \lambda_{LSPR} - 500 \tag{1}$$

Therefore, the calculated AuNP sizes were 5 nm, 18 nm, and 7 nm for Exp-1, Exp-2, and Exp-3, respectively. The shape and size of the AuNPs in Exp-1 were confirmed by TEM images as displayed in Fig. 5b.

Figure 6 shows visual appearance and measured extinction spectra of colloidal AuNPs before and after Cr(VI) test was performed. Extinction spectra of BSA-AuNPs appears to be slightly redshifted from those of as-prepared AuNPs. BSA is needed to maintain stability of AuNPs in strong acid solution after addition of HBr, which was added prior to Cr(VI) introduction to the test solution. HBr is essential to lower the electron potential of Au(I)/Au(0) and increase the electron potential of Cr(VI)/Cr(III) [8]. The standard electron potentials of Au(I)/Au(0) and Cr(VI)/Cr(III) are 1.691 eV and 1.33 eV, respectively, which make it impossible for Cr(VI) to oxidize AuNP surface directly. However, in the presence of bromide ions, the electron potential of Au(I)/Au(0) decreases to 0.959 eV [18], and AuNPs are readily oxidized by Cr(VI) ions. The etching of AuNPs caused the pink, purplish pink,

and red colors of the colloidal solution to fade-away (Fig. 6a-6c) and the extinction spectra to show lower intensities (Fig. 6d-6f).

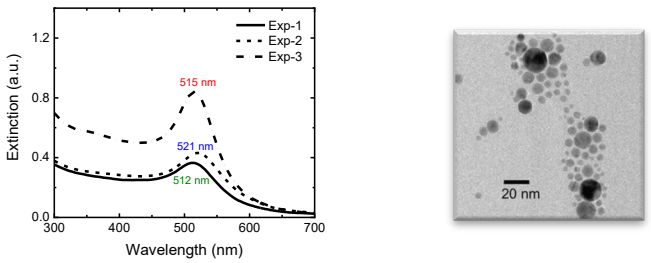

(a) (b)

Fig. 5. (a) Extinction spectra of AuNPs fabricated via laser-induced photochemical reduction. (b) TEM image of AuNPs produced by 15 minutes irradiation of 0.125 mM Au^{3+} solution.

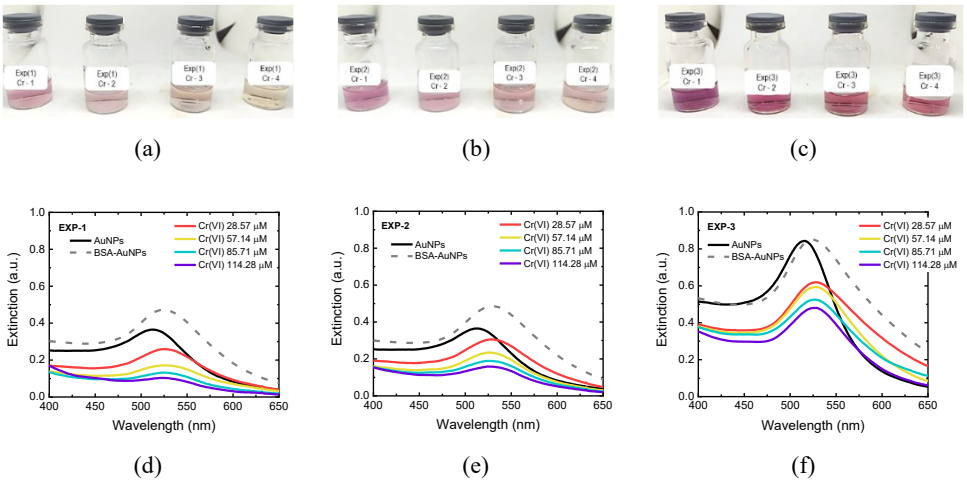

(a) (b) (c)

(d) (e) (f)

Fig. 6. Visual appearance and extinction spectra of colloidal solution containing (a, d) small AuNPs with low Au concentration, (b, e) large AuNPs with low Au concentration, and (c, f) small AuNPs with high Au concentration before and after Cr(VI) introduction.

The λ_{LSPR} shift and measured extinction change as functions of Cr(VI) concentration are shown in Fig. 7a and 7b. The λ_{LSPR} shift per Cr(VI) concentration ($\Delta \lambda_{LSPR}$ /[Cr(VI)]) for Exp-1, Exp-2, and Exp-3 were 0.00 nm/μM , 0.05 nm/μM, and 0.02 nm/μM, respectively. The higher $\Delta\lambda_{LSPR}$/[Cr(VI)] shown by Exp-2 implied better $\Delta\lambda_{LSPR}$ resolution, demonstrated by the more distinct color change shown (from purplish pink to almost transparent). Since spherical AuNPs have λ_{LSPR} only in visible range, the resolution would be limited at some point. In this case, the use of anisotropic AuNPs with λ_{LSPR} in the near infrared range would be a better choice. Next, the extinction change per Cr(VI) concentration (ΔExt/[Cr(VI)]) for Exp-1, Exp-2, and Exp-3 were 0.0018/μM, 0.0017 nm/μM, and 0.0017 nm/μM, respectively. The similar values complied with the finding from simulation study, where the detected analyte concentration correlated to the total AuNP volume loss. Thus, Au concentration did not affect the extinction peak value. Meanwhile, the higher intercept value of Exp-3 (0.676), compared to those of Exp-1 (0.293) and Exp-2 (0.344), suggested possibility to reach lower detection limit when higher concentration of Au is used.

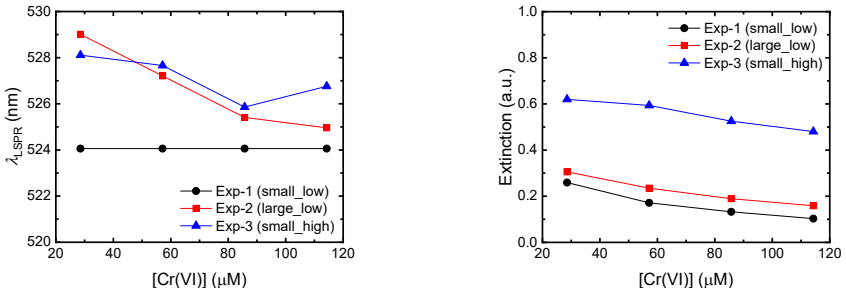

Fig. 7. (a) LSPR wavelength and (b) measured extinction peak as a function of Cr(VI) concentration.

4 Conclusion

Both simulation and experiment results agree that, in etching-based Cr(VI) sensing, large AuNPs displayed better λ_{LSPR} resolution compared to small nanoparticles. This would be demonstrated by the wider shift in color spectrum. On the other hand, though Au concentration affect the colloidal solution extinction peak and color intensity, concentration of AuNPs does not significantly contributes to the degree of intensity change. However, higher concentration of AuNPs offered higher Cr(VI) sensing range, i.e. lower detection limit. More investigation are still needed to learn the effect of size and concentration of anisotropic AuNPs to the etching-based detection. It is also of interest to learn their effect to the non-etching based detection.

Acknowledgements

This work was supported by Directorate of Research and Development, Universitas Indonesia under *Hibah Publikasi Terindeks International* (PUTI) Q2 2023. The authors also acknowledge the laser facility at the Research Center for Photonics, National Research and Innovation agency of Indonesia (BRIN) as well characterization support from ELSA BRIN.

References

1. M. Tumolo et al., Int. J. Environ. Res. Public Health **17**, 5438 (2020).
2. F. Séby, S. Charles, M. Gagean, H. Garraud, and O. F. X. Donard, J. Anal. At. Spectrom. **18**, 1386 (2003).
3. Z. Sun and P. Liang, Microchim. Acta **162**, 121 (2008).
4. I. Tsuyumoto and Y. Maruyama, Anal. Chem. **83**, 7566 (2011).
5. C. Dong et al., Dalt. Trans. **45**, 8347 (2016).
6. S. Li et al., Colloids Surfaces A Physicochem. Eng. Asp. **535**, 215 (2017).
7. V. Amendola, R. Pilot, M. Frasconi, O. M. Maragò, and M. A. Iatì, J. Phys. Condens. Matter **29**, 203002 (2017).
8. J. F. Guo et al., Anal. Methods **8**, 5526 (2016).
9. F.-M. Li et al., Sensors Actuators B Chem. **155**, 817 (2011).

10. J. L. Montaño-Priede, M. Sanromán-Iglesias, N. Zabala, M. Grzelczak, and J. Aizpurua, ACS Sensors **8**, 1827 (2023).
11. Ž. Krpetić et al., Small **8**, 707 (2012).
12. U. Hohenester and A. Trügler, Comput. Phys. Commun. **183**, 370 (2012).
13. U. Hohenester, Comput. Phys. Commun. **222**, 209 (2018).
14. P. B. Johnson and R. W. Christy, Phys. Rev. B **6**, 4370 (1972).
15. T. Nakamura et al., AIP Adv. **3**, 082101 (2013).
16. T. Nakamura, Y. Mochidzuki, and S. Sato, J. Mater. Res. **23**, 968 (2008).
17. N. G. Khlebtsov, Anal. Chem. **80**, 6620 (2008).
18. J. Xin et al., Talanta **101**, 122 (2012).